Обзор ArXiv: astro-ph, 8-12 апреля 2019 года

От Сильченко О.К.

ArXiv: 1904.04222

Inner and outer rings are not strongly coupled with stellar bars

S. Díaz-García[1,2], S. Díaz-Suárez[1,2], J. H. Knapen[1,2,3], and H. Salo[4]

[1] Instituto de Astrofísica de Canarias, E-38205, La Laguna, Tenerife, Spain
e-mail: simondiazgar@gmail.com
[2] Departamento de Astrofísica, Universidad de La Laguna, E-38205, La Laguna, Tenerife, Spain
[3] Astrophysics Research Institute, Liverpool John Moores University, IC2, Liverpool Science Park, 146 Brownlow Hill, Liverpool, L3 5RF, UK
[4] Astronomy Research Unit, University of Oulu, FI-90014 Finland

Received 13 March 2019; accepted 8 April 2019

ABSTRACT

Rings are distinctive features of many disk galaxies and their location and properties are closely related to the disk dynamics. In particular, rings are often associated to stellar bars, but the details of this connection are far from clear. We study the frequency and dimensions of inner and outer rings in the local Universe as a function of disk parameters and the amplitude of non-axisymmetries. We use the 1320 not-highly inclined disk galaxies ($i < 65°$) from the S^{4}G survey. The ring fraction increases with bar Fourier density amplitude: this can be interpreted as evidence for the role of bars in ring formation. The sizes of inner rings are positively correlated with bar strength: this can be linked to the radial displacement of the 1/4 ultra-harmonic resonance while the bar grows and the pattern speed decreases. The ring intrinsic ellipticity is weakly controlled by the non-axisymmetric perturbation strength: this relation is not as strong as expected from simulations, especially when we include the dark matter halo in the force calculation. The ratio of outer-to-inner ring semi-major axes is uncorrelated with bar strength: this questions the manifold origin of rings. In addition, we confirm that i) approximately $\sim 1/3$ and $\sim 1/4$ of the non-barred galaxies in the S^{4}G host inner and outer rings, respectively; ii) on average, the sizes and shapes of rings are roughly the same for barred and non-barred galaxies; and iii) the fraction of inner (outer) rings is a factor of 1.2 – 1.4 (1.65 – 1.9) larger in barred galaxies than in their non-barred counterparts. Finally, we apply unsupervised machine learning (Self-Organizing Maps, SOMs) to show that, among early-type galaxies, ringed or barred galaxies cannot be univocally distinguished based on 20 internal and external fundamental parameters. We confirm, with the aid of SOMs, that rings are mainly hosted by red, massive, gas-deficient, dark-matter poor, and centrally concentrated galaxies. We conclude that the present-day coupling between rings and bars is not as robust as predicted by numerical models, and diverse physical mechanisms and timescales determine ring formation and evolution.

Key words. galaxies: structure - galaxies: evolution - galaxies: statistics - galaxies: spiral - galaxies: fundamental parameters -

Выборка

- S4G
- 1320 галактик с i<65deg, из них:
- 825 с барами
- 465 с внутренними кольцами
- 264 с внешними кольцами
- 103 с обоими кольцами

Кольца – в массивных галактиках

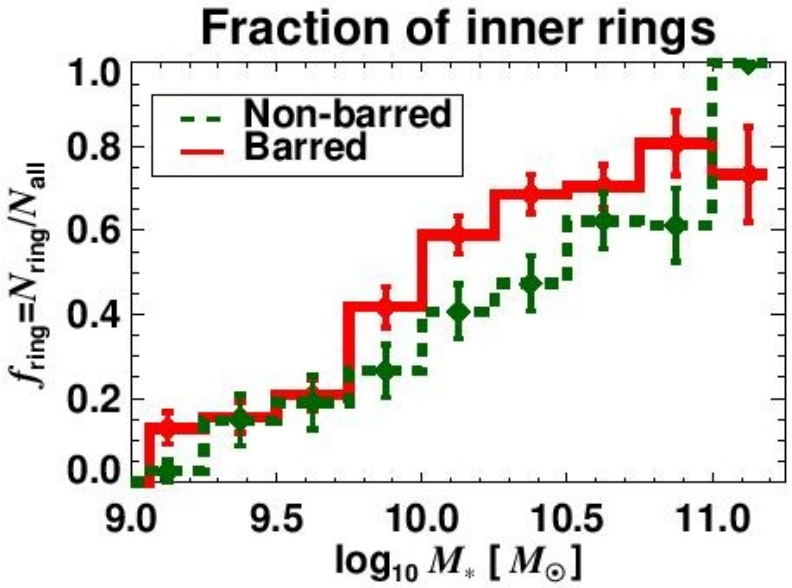

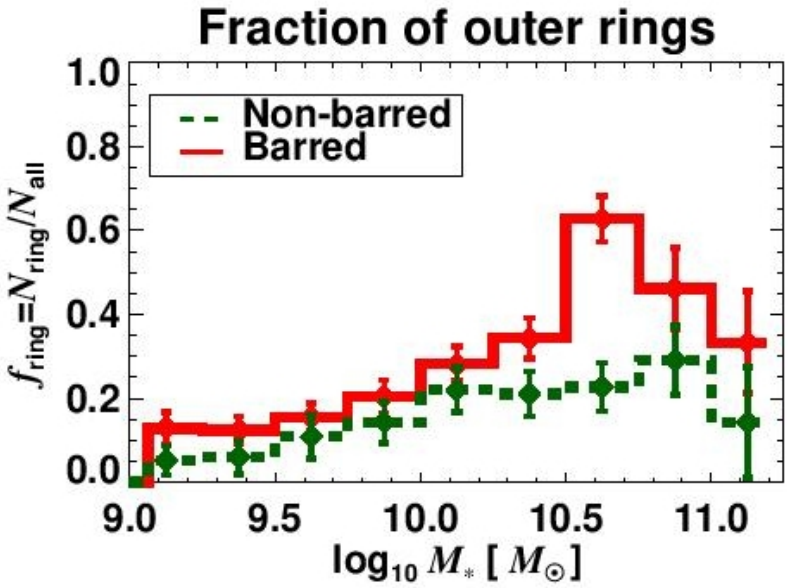

…и немного чаще и больше - в барных галактиках ранних типов

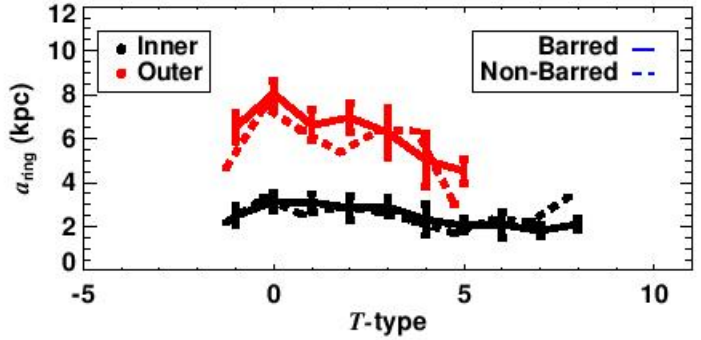

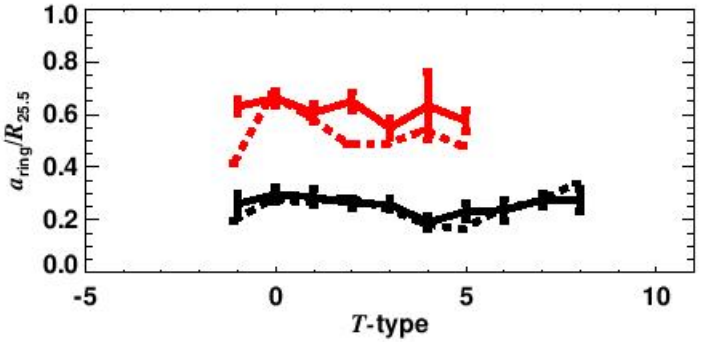

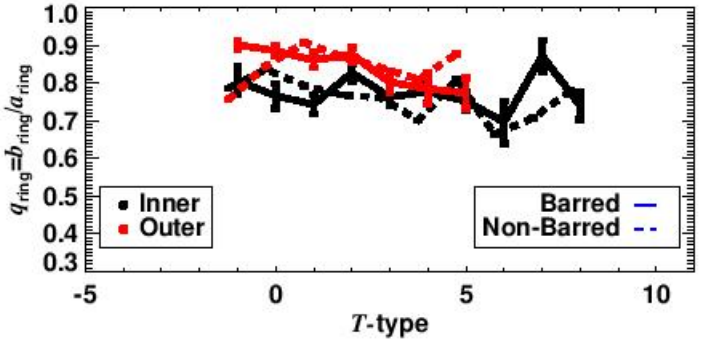

Есть ли связь с силой бара?

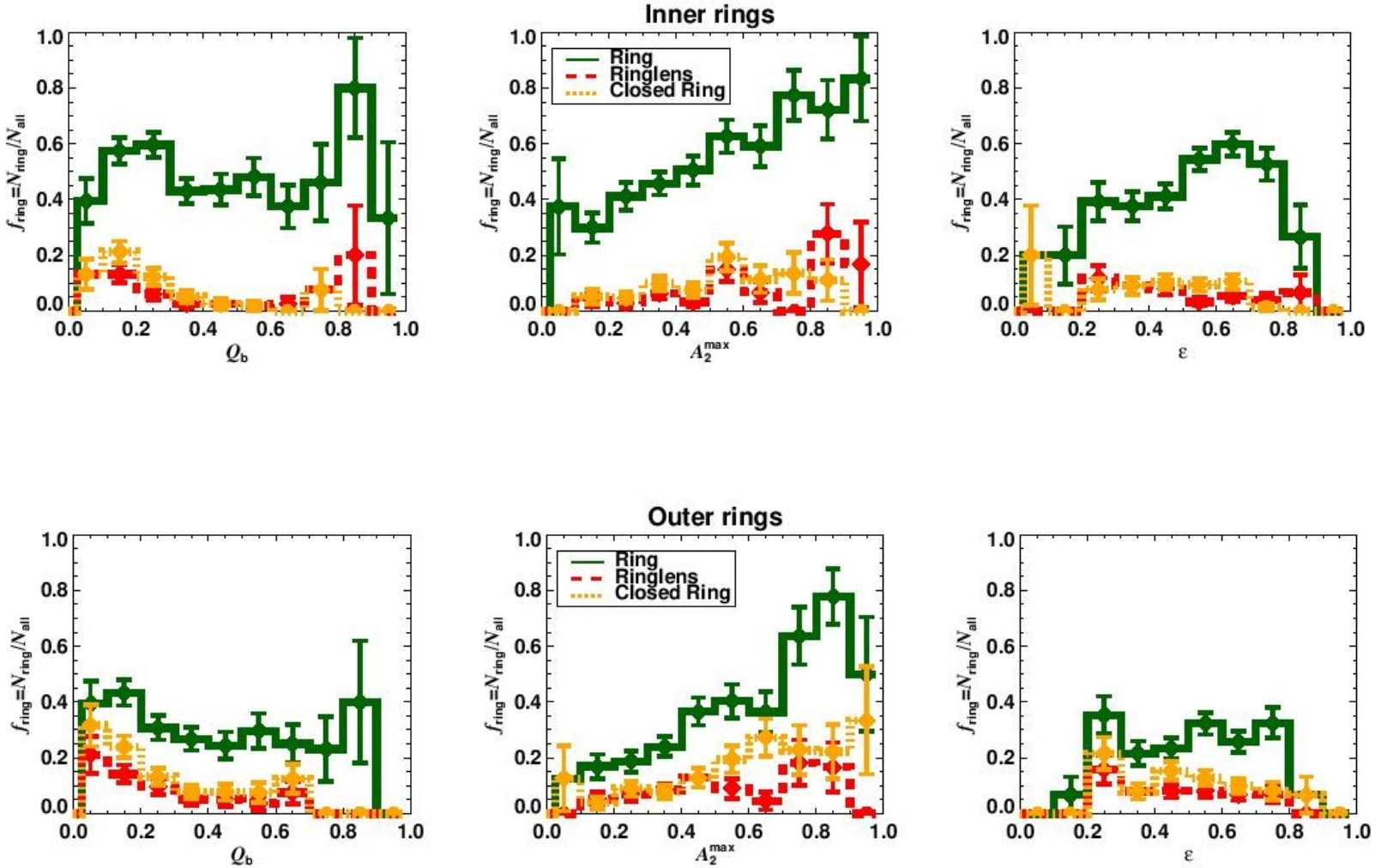

Размер связан с силой бара только для внутренних колец

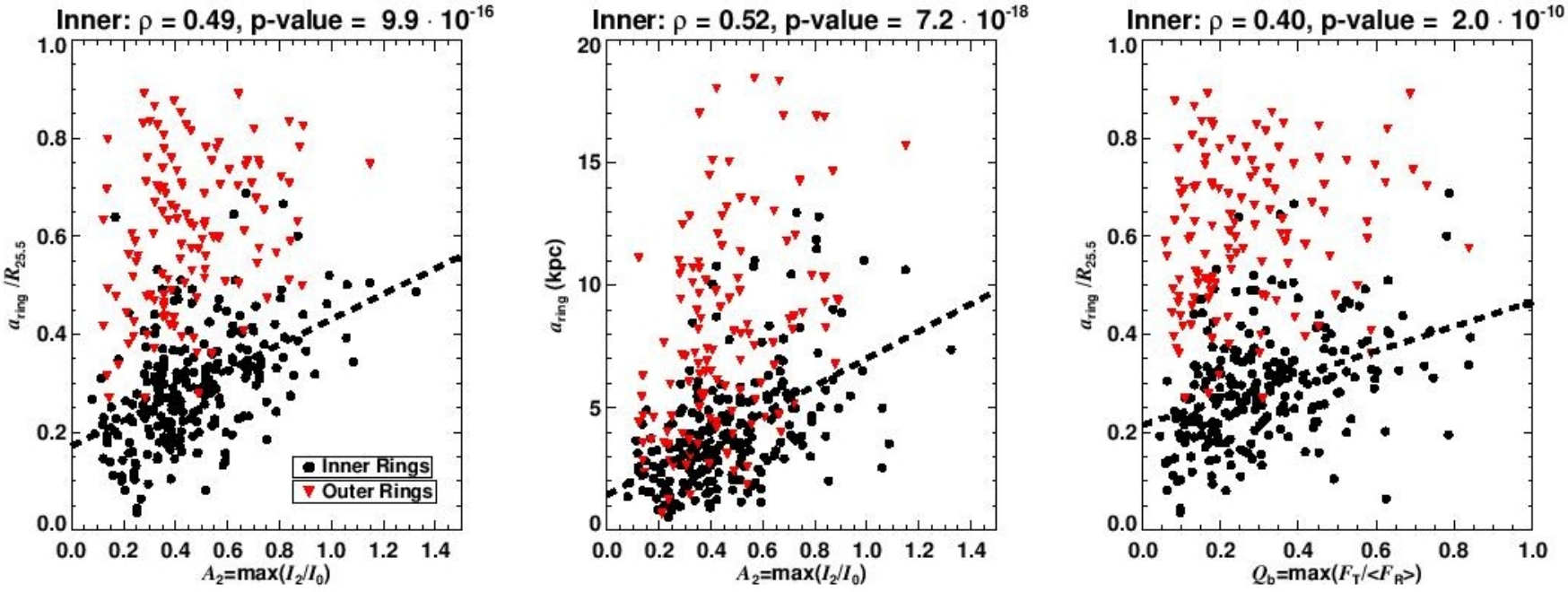

Fig. 6. De-projected semi-major axis of rings, normalised to $R_{25.5}$ and in physical units, as a function of the bar strength, estimated from the $m = 2$ bar Fourier amplitude (*left and central panels*). The disk-relative sizes of rings are also compared to the bar torque parameter (*right panel*). The colour palette is the same as in Fig. 2, separating inner and outer rings. The Spearman's correlation coefficient and significance of the correlation for the inner rings is shown above the figures. The dashed black line corresponds to the linear fit to the cloud of points for the inner rings.

Если кольца сидят на резонансах, то на каких? Разброс отношений размеров внутренних и внешних…

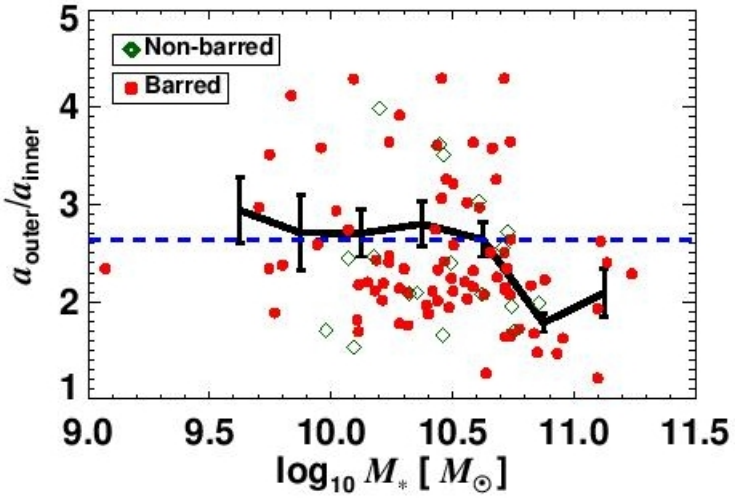

Fig. 9. Ratio of the de-projected semi-major axes of outer and inner rings versus the total stellar mass of the host galaxy, for a subsample of 103 galaxies. The horizontal dashed blue line corresponds to the expected ratio for a galaxy with a flat rotation curve and a linear treatment of its resonances (see text). With a black line we show the running mean and standard deviation of the mean, in bins of 0.25 dex. Barred and non-barred galaxies are shown with different colours and symbols.

Under the assumption of a flat rotation curve, the linear treatment of resonances implies that $R_{OLR}/R_{CR} = 1 + \sqrt{2}/2$ and $R_{UHR}/R_{CR} = 1 - \sqrt{2}/4$ (e.g. Binney & Tremaine 1987), where R_{OLR}, R_{UHR} and R_{CR} refer to the location of the outer Lindblad resonance, the inner ultraharmonic resonance, and the corotation radii, respectively. This implies that $R_{OLR}/R_{UHR} \approx 2.64$, which is consistent with the mean values that we obtain for a_{outer}/a_{inner} (Fig. 9). Note that a_{outer}/a_{inner} tends to be slightly lower than 2.64 for all the data points with $M_* > 10^{10.75} M_\odot$ (13 galaxies). This, and the fairly large scatter in the plot, can be due to differences in the mass distribution and shape of the rotation curves of each of the galaxies (e.g., declining rotation curves among the most massive galaxies). Alternatively, these could be partly explained by the fact that some outer rings might not form exactly at the OLR, but at the outer 1:4 resonance (Buta 2017b).

Закрывают манифолды: антикорреляция вместо корреляции

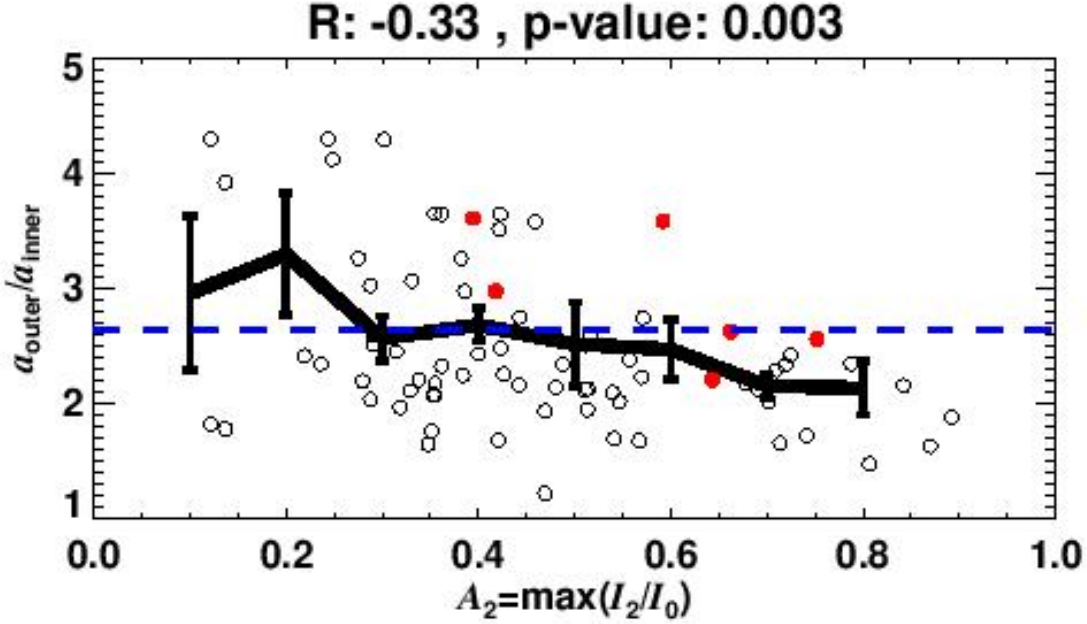

ArXiv: 1904.04366

The Neutral Gas Properties of Extremely Isolated Early-Type Galaxies III

Trisha Ashley,[1,2] Pamela M. Marcum,[2] Mehmet Alpaslan,[3] Michael N. Fanelli,[2] and James D. Frost

[1] *Space Telescope Science Institute*
[2] *NASA Ames Research Center*
[3] *New York University*

ABSTRACT

We report on the neutral hydrogen gas content (21-cm emission) of eight extremely isolated early-type galaxies (IEGs) using the Green Bank Telescope. Emission is detected in seven of the eight objects. This paper is the third in a series that collectively present new H I observations for 20 IEGs. Among the 14 H I detections in our observations, eight exhibit a Gaussian-like H I line profile shape, four are double-peaked, one is triple-peaked, and another has a plateaued rectangular shape. Five additional IEGs observed in previous surveys were added to our analysis, bringing the total number of IEGs with H I observations to 25. Of these objects, emission is detected in 19 (76%). The 25 IEGs in our combined study have gas masses that are systematically larger than their luminosity-matched comparison galaxy counterparts. The isolated early-type galaxies presented here follow a trend of increasing gas-richness with bluer B−V colors. This correlation is also observed in a comparison sample drawn from the literature composed of loose group and field early-type galaxies. Two IEGs, KIG164 and KIG870, exhibit properties highly anomalous for spheroidal systems: luminous (M_B = −20.5, −20.1) and blue (B−V = 0.47, 0.48) respectively, with substantial neutral gas, M_{HI} = 4.1 & 5.5 $\times 10^9$ $M_\odot$. Other IEG systems may represent early-type galaxies continuing to assemble via quiescent H I accretion from the cosmic web or relaxed merged systems.

Выборка

The sample of extremely isolated early-type galaxies presented here is drawn from the compilations of Marcum et al. (2004) and Fuse et al. (2012) (M04 & F12). An "early-type" morphology was assigned to galaxies with bulge-to-total light ratios (B/T) of ≥ 0.6 (Marcum et al. 2004) or inverse concentration index ratios (R_{50}/R_{90}) of $\leq$0.38 (Fuse et al. 2012), resulting in a dataset including both elliptical and S0 galaxies ($-5 < T \leq -1$). The parent samples were chosen to be separated by at least 2.5 Mpc in co-moving distance from neighboring galaxies brighter than $M_V = -16.5$ ($\sim$2 magnitudes dimmer than ATLAS 3D), eliminating the possibility of past interactions with any non-dwarf companions (Aars et al. 2001). Using deep optical images, M04 & F12 found evidence of past interactions and mergers in several of the IEGs, including asymmetric outer isophotes and multiple nuclei. The M04 sample was drawn from the Catalog of Isolated Galaxies (Karachentseva 1973) and contains nine IEGs brighter than $M_B < -19.6$ with a range of colors, $0.46 < B-V < 0.96$. The larger F12 sample, extracted from the Sloan Survey, is on average bluer in color, less luminous, and smaller in physical extent than the M04 set, with av-

Примеры из ярких

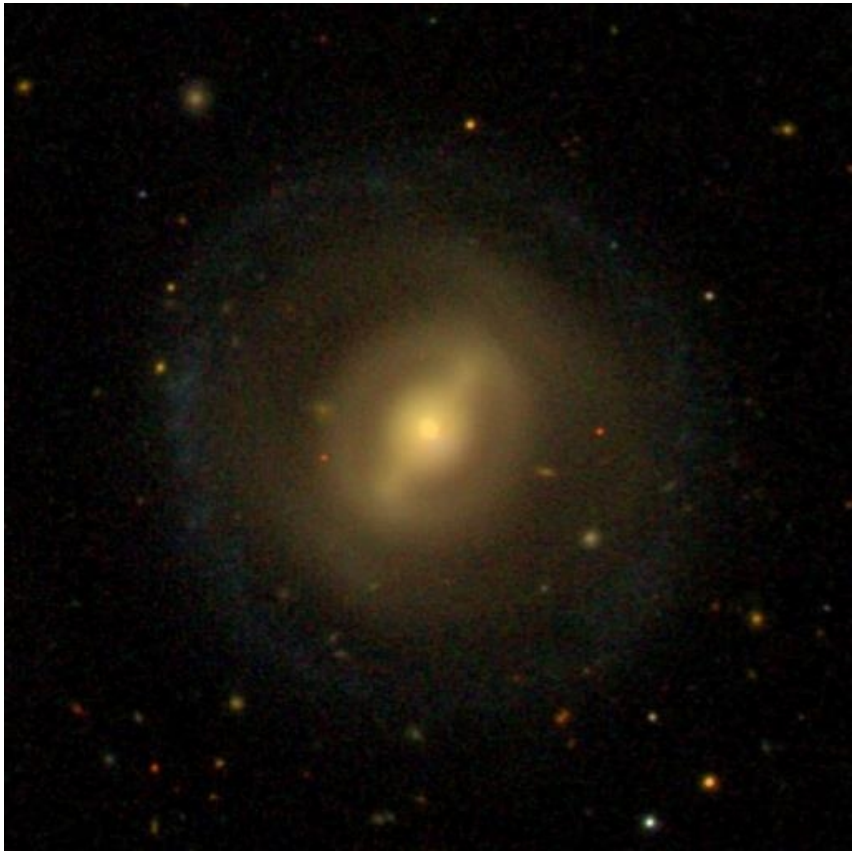

NGC 1211

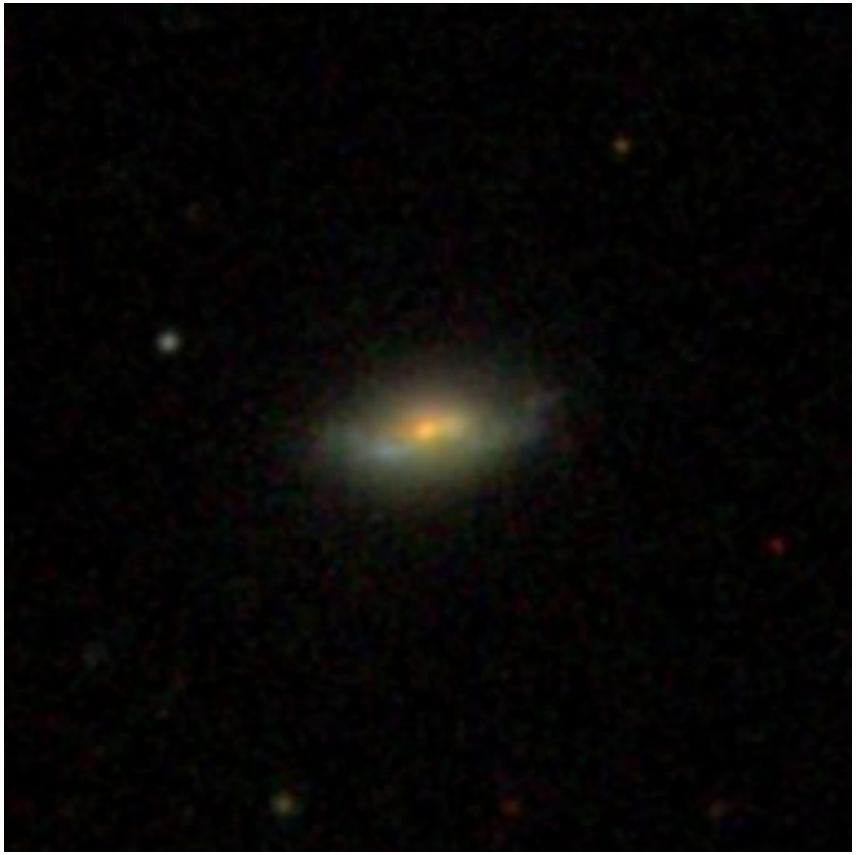

SBS 1327+597

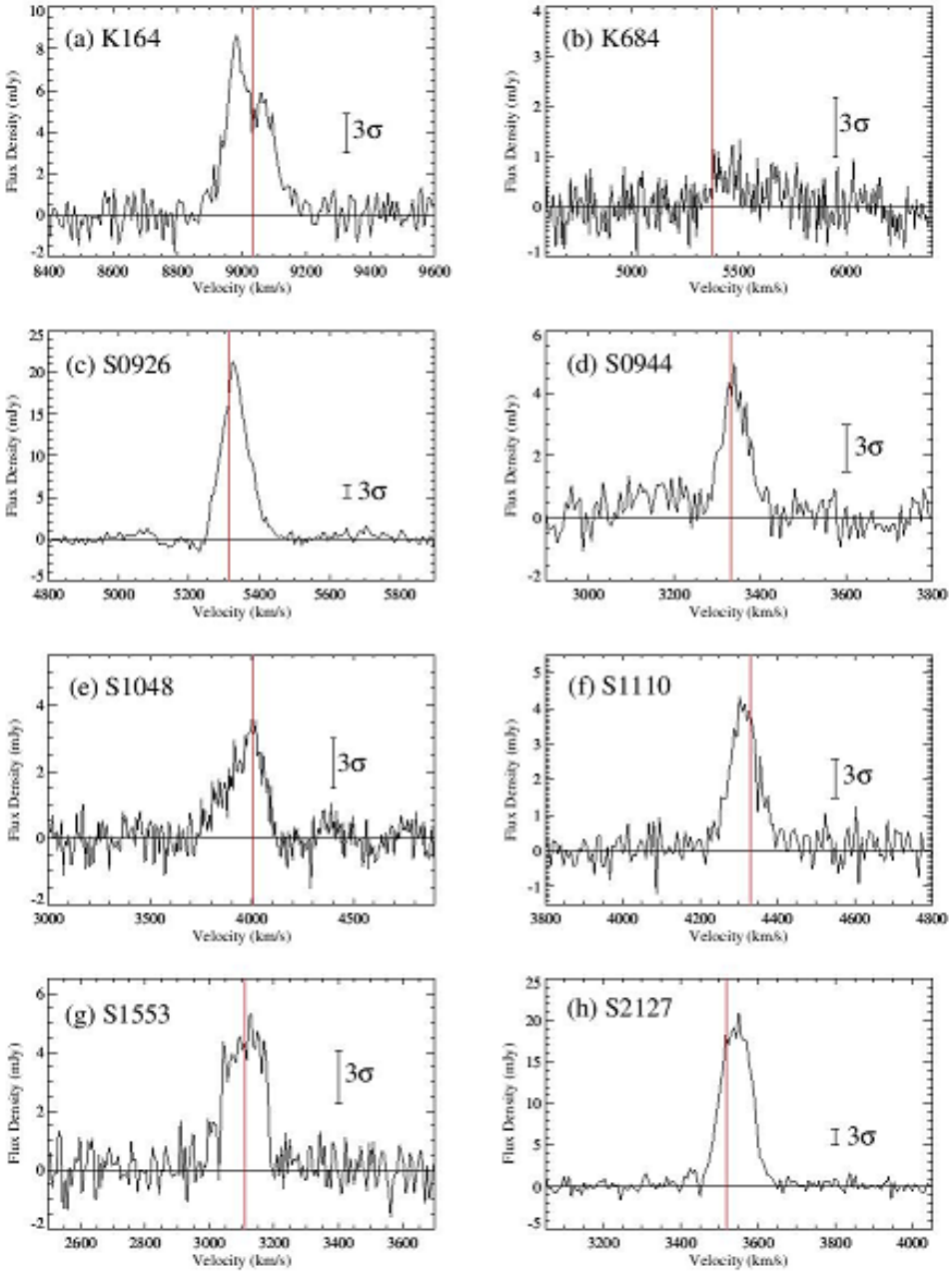

Figure 1. H I line profiles for the 8 IEGs reported here. Source names are given in the upper left corner, shortened for brevity. The red vertical lines indicate the optically defined systemic recessional velocity for each galaxy, sourced from NED. Error bar lengths are 3 times the rms per channel. These profiles have been Hanning and boxcar-smoothed resulting in a 6.9 km s^{-1} channel width.

а это - не сигнал?..

Нормальное отношение массы газа к светимости…

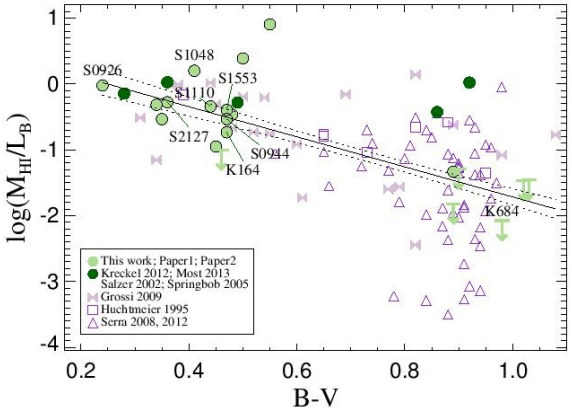

Figure 2. B−V vs. $\log(M_{HI}/L_B)$ for the entire IEG sample contrasted with the comparison sample. Data presented here and in Ashley et al. (2017, 2018) are shown in filled light green circles. Data for IEGs Mrk737, SDSSJ122123.13+393659.5, SBS1327+597, SDSSJ132337.69+291717.1 and NGC1211 obtained from, respectively Salzer et al. (2002), Kreckel et al. (2012) (2), Most et al. (2013) and Springob et al. (2005) are displayed in dark green. Data points centered directly under, above or linked to abbreviated galaxy names indicate the 8 new objects presented in this paper. Green arrows represent 5σ upper mass limits for non-detections of IEGs. The comparison ETG sample is shown in purple with the symbol indicating the published source. The linear relationship (black solid line) includes both the detected IEGs and comparison galaxies; dashed line the $\pm1\sigma$ envelop.

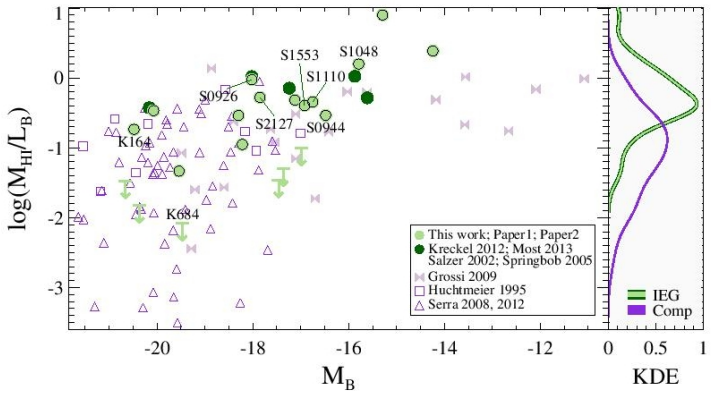

Figure 3. Left panel: The log of the H I mass-to-blue luminosity ratio vs. absolute blue magnitude for the IEG and comparison samples. The same color coding is used as in Figure 2. **Right panel:** The kernel distribution estimation of the IEG (green) and comparison (purple) $\log(M_{HI}/L_B)$ distributions. This analysis includes only those galaxies having measured H I fluxes ($S_{HI} \geq 0.28$ Jy km s^{-1}) that would have been detectable by our survey constraints. An offset between the IEG and comparison sample distributions is apparent.

… но масса газа у изолированных все же больше!

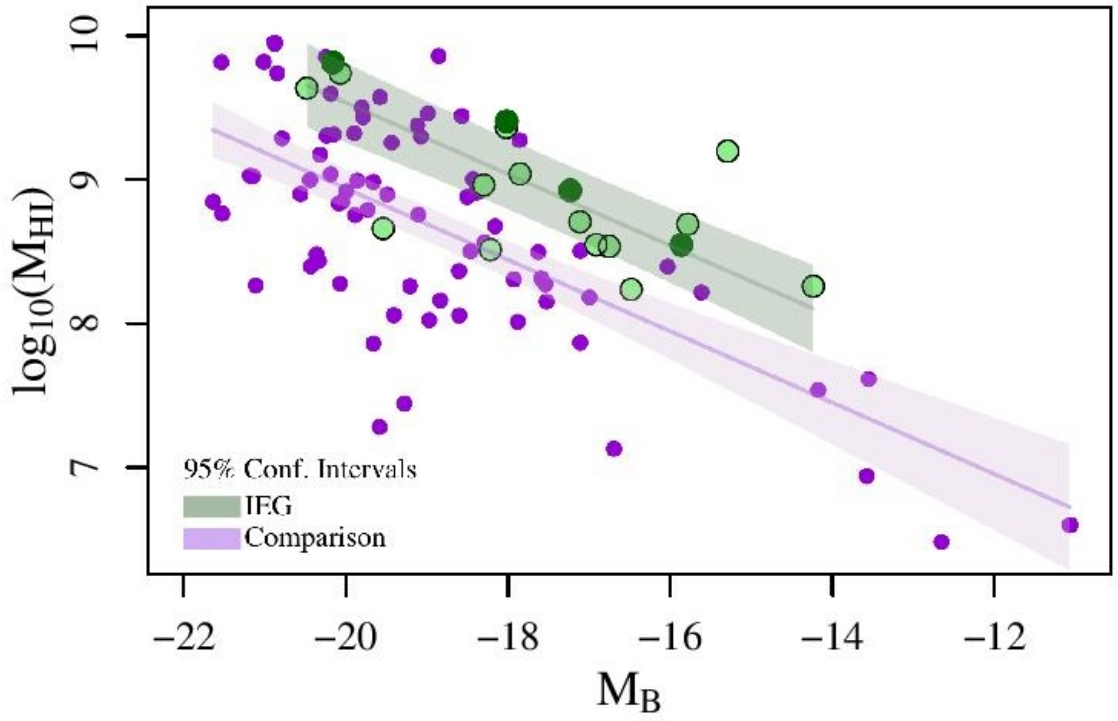

Figure 4. Statistical analyses: The log of the H I-mass vs. absolute blue magnitude with same color legend as Figure 2 and displaying the same dataset ued to construct the KDEs displayed in Figure 3, e.g. those galaxies having $S_{HI} \geq 0.28$ Jy km s^{-1} for statistical analysis having the same color legend as Figure 3. The fitted lines display the results of linear regression analysis; shaded regions are the 95% confidence intervals for the IEG and comparison samples. The analysis supports the hypothesis that the H I mass distributions of the two samples are distinct.